Role of the Coordination of the Azido Bridge in the Magnetic Coupling of Copper(II) Binuclear Complexes

Jesús Cabrero,[a] Coen de Graaf,[a] Esther Bordas,[a] Rosa Caballol,*[a] and Jean-Paul Malrieu[b]

In memory of Olivier Kahn

Abstract: It is well-known that the azido bridge gives rise antiferromagnetic (AF) or ferromagnetic (F) coupling depending on its coordination mode, namely end-to-end or end-on, respectively. The aim of the present work is to analyse the factors contributing to this different magnetic behaviour. The difference dedicated configuration interaction (DDCI) method is applied to several binuclear Cu^{II} azido-bridged models with both types of coordination. In end-on complexes, the direct exchange and the spin polarisation contributions are found to be responsible for the ferromagnetic coupling. In end-to-end complexes, both the direct exchange and the spin polarisation are small and the leading term is the antiferromagnetic dynamical polarisation contribution. The most relevant physical effects are included in the DDCI calculations so that good quantitative agreement is reached for the coupling constant as well as the spin densities.

Keywords: ab initio calculations · binuclear complexes · copper · magnetic properties · N ligands

Introduction

In the last few decades, the magnetic behaviour of polynuclear transition-metal complexes has been extensively studied. Among them, ligand-bridged Cu^{II} binuclear complexes are a privileged class that has merited a large part of these studies. The great versatility of bridging and external ligands coordinated to copper has led to a wide range of metal coordination geometries. The large amount of information on structures and magnetic behaviour has prompted investigations of magneto-structural correlations.[1, 2] The biradical character of these systems, which arises from the d^9 configuration of Cu^{II}, has also stimulated theoreticians to test their methodologies in the calculation of the magnetic exchange coupling constant J, and to investigate the origin of the magneto-structural correlations.

Anderson[3] interpreted J as the balance of two antagonist contributions, $J = J_F + J_{AF}$, where F and AF indicate ferromagnetic and antiferromagnetic contributions, respectively. J_F is attributed to the direct exchange between the electron spin of the magnetic centres (always ferromagnetic, i.e. stabilising the triplet state), and J_{AF} is interpreted through the delocalisation effect that can only occur in the singlet state (hence antiferromagnetic). In the early 1970s, Hay, Thibeault and Hoffmann[4] as well as Kahn and Briat[5] proposed similar qualitative models that have been applied to binuclear copper complexes[6–11] to explain the trends of the coupling constant with respect to geometrical variations and the role of the ligands. Ab initio perturbative calculations of the singlet–triplet separation in a series of complexes[12, 13] gave the first quantitative estimations. The broken symmetry approach based on Noodleman's[14] expression has been extensively used to calculate J from the unrestricted triplet and the broken symmetry solution, particularly coupled with density functional theory (DFT) methods.[8, 9, 11, 15–18] Ab initio configuration interaction (CI) calculations, especially within the difference dedicated CI (DDCI) approach[19] have also been performed for a number of binuclear Cu^{II} complexes[20–22] as well as for copper oxide insulators.[23–26]

That azido-bridged Cu^{II} complexes present two coordination modes with different magnetic behaviour has inspired a lot of experimental[27–35] and theoretical work.[8, 11, 17, 18, 36] It is

[a] Prof. R. Caballol, Dr. J. Cabrero,
Dr. C. de Graaf, E. Bordas
Departament de Química Física i Inorgànica
and Institut d'Estudis Avançats
Universitat Rovira i Virgili
Pl. Imperial Tarraco, 1, 43005 Tarragona (Spain)
Fax: (+34) 977-559-563
E-mail: caballol@quimica.urv.es

[b] Prof. J.-P. Malrieu
Laboratoire de Physique Quantique, IRSAMC
Université Paul Sabatier
118, route de Narbonne, 31062 Toulouse Cédex (France)

Supporting information for this article is available on the WWW under http://www.chemeurj.org or from the author.

 DOI: 10.1002/chem.200204167

now well-established that the end-to-end (ete) coordination gives antiferromagnetic complexes, whereas the end-on (eo) coordination gives ferromagnetic coupling. The strong dependence of the antiferromagnetic exchange coupling on the structural parameters in end-to-end complexes has been discussed from one-electron arguments.[11] The coordination geometry of the copper ions can vary between the two square pyramids represented in Figure 1. The distortion induces a

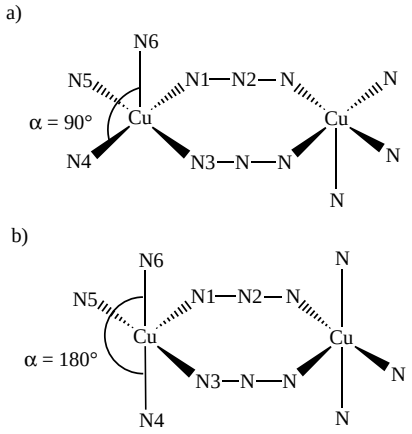

Figure 1. Schematic representation of the two square-pyramidal coordinations in end-to-end azido-bridged Cu^{II} complexes: a) coordination with two azido ligands in equatorial positions; b) coordination with one azido ligand in the apical position.

change in the magnetic orbitals, and consequently in the value of the coupling constant. However, theoretical studies of such systems should not be restricted to the mere reproduction of the magneto-structural dependencies but must be extended to the interpretation of the mechanisms that could explain the different behaviour of both coordination modes. Charlot and co-workers[36] proposed that the spin polarisation is the main factor for the difference between end-on and end-to-end complexes, that is, it stabilises the triplet state with respect to the singlet state in the end-on coordination and stabilises the singlet state with respect to the triplet state in the end-to-end complexes.[36] In addition, valence bond configuration interactions (VBCIs),[37] which use parameters that have been carefully fitted from spectroscopic information, also suggests the spin polarisation plays an important role in the ferromagnetic behaviour of the end-on complexes.[35]

Our aim with the present work is to accurately estimate the trend of the exchange coupling constants versus the structural parameters for some azido-bridged complexes in the end-to-end and end-on coordination modes, and to give an analysis of the main factors responsible for their magnetic behaviour. We will demonstrate that DDCI is able to include the most relevant physical effects of the exchange coupling both in antiferromagnetic and ferromagnetic azido-bridged Cu^{II} binuclear complexes to such an extent that good quantitative agreement is reached both for the coupling constant and the spin densities.

The effect of the external ligands has been studied as well as the effect of the correlation of the bridge orbitals that seems to be crucial to obtain correct magnetic couplings and spin densities in end-on complexes. The main contributions leading to the antiferromagnetic coupling in end-to-end complexes and to the ferromagnetic behaviour in the end-on ones are discussed. As the spin densities for a ferromagnetic end-on complex have been reported[34] from polarised neutron diffraction data, we have also calculated these values for comparison.

Theoretical framework: In the particular case of Cu^{II} dinuclear complexes, the phenomenological Heisenberg–Dirac–Van Vleck Hamiltonian[38] takes the simple form given in Equation (1), where $\hat{S_1}$ and $\hat{S_2}$ are total spin operators.

$$\hat{H} = -2J\hat{S_1}\hat{S_2} \tag{1}$$

From this, it is straightforward to derive that J is given by the singlet–triplet energy difference: $\Delta E_{ST} = E_S - E_T = 2J$, where the coupling constant J is negative for antiferromagnetic coupling and positive for ferromagnetic coupling. In DFT methods, Noodleman's procedure is commonly used,[14, 39] where the singlet energy is approximated from the broken symmetry (BS) solution. The expression for the singlet–triplet gap may be written as Equation (2), where S_{ab} is the overlap between the magnetic orbitals in the broken symmetry calculation.[17, 39–41]

$$2J = \Delta E_{ST} = \frac{2(E_{BS} - E_T)}{1 + S_{ab}^2} \tag{2}$$

Since the distance between the magnetic centres is usually rather large, S_{ab}^2 is small and it is, in general, relevant to evaluate the S–T gap as in Equation (3).[40]

$$2J = \Delta E_{ST} \sim 2(E_{BS} - E_T) \tag{3}$$

Recent theoretical work on the magnetic coupling in azido-bridged Cu^{II} complexes use DFT approaches for the extraction of the magnetic coupling constant. The structural dependencies in complexes with end-to-end as well as end-on coordination have been studied with the B3LYP functional.[8, 11]

The DDCI method: The difference dedicated configuration interaction (DDCI) method[19] has proved to give accurate evaluations of the exchange magnetic coupling in the recent past.[21, 22, 42, 43] The method starts with the selection of a model space built with the configurations that play a major role in the energy difference, namely, the complete active space (CAS) generated with the molecular orbitals (MOs) implied in the transition. In the case of dinuclear Cu^{II} systems, the (2,2) CAS is generated by distributing two electrons in all possible ways over two active molecular orbitals, the bonding and antibonding combinations of the magnetic orbitals at each centre, a and b. The CAS may as well be expressed in terms of localised contributions generated from the magnetic orbitals, that is, the neutral $|a\bar{b}\rangle$ and $|b\bar{a}\rangle$ and the ionic $|a\bar{a}\rangle$ and $|b\bar{b}\rangle$determinants in the valence bond (VB) context.

The DDCI space includes the determinants of the CAS and the double excitations on the top of them with at least one active orbital, that is, a subspace of the CAS single and

doubles configuration interaction. The application of DDCI to magnetic systems ensures the inclusion of all relevant physical effects as potential exchange, kinetic exchange, dynamical spin polarisation, charge transfer and other important electron correlation effects as described in a recent article.[22a]

The most important characteristics of the DDCI method can be summarised in the following points: 1) since it is a variational method, it allows the external correlation to modify the coefficients of the CAS; 2) the DDCI matrix is invariant under rotations of the MOs in the active, doubly occupied or virtual subsets, and therefore it is equivalent to work with magnetic (localised) orbitals or with symmetry-adapted MOs; and 3) the number of determinants in the DDCI space is proportional to the third power of the MOs set, instead of the fourth power, as in a CAS*SDCI calculation.

In most of our recent applications of the DDCI technique, we systematically improved the active MOs by the use of mean natural orbitals (NO).[21, 22, 44, 45] The mean density matrix $\bar{R} = (R_S + R_T)/2$ (where R_S and R_T are the density matrices for the singlet and triplet state, respectively) is diagonalised to obtain mean natural orbitals. By iterating the process to convergence, DDCI becomes the IDDCI technique.[46] As previously shown,[44, 47] the iteration of the MOs improves the active orbitals and increases the norm of the projection of the C_i vector onto the CAS. Furthermore, if some inactive orbitals have significant fractional occupations, it suggests that they should be included in the active space.

Computational Methods

Several series of DDCI calculations were performed for both end-to-end (ete) and end-on (eo) Cu^{II} doubly azido-bridged complexes. In the end-to-end pentacoordinated complexes, the aza-cyclic external ligands were modelled by three NH_3 groups: $[(NH_3)_6Cu_2(\mu\text{-}1,3\text{-}N_3)_2]^{2+}$. A first set of calculations was performed on highly symmetrised structures that correspond to the two limiting square pyramids represented in Figure 1. The structural parameters for these two structures were taken from the most similar crystallographic structure in each case. The two models either have two azido ligands in the basal plane (Figure 1a; ete-m1) or one azido ligand in the apical position (Figure 1b; ete-m2). The second set of calculations was performed on five distorted bridging geometries, taken from to the crystallographically determined structures of the compounds **1** to **5**: $[L_2Cu_2(\mu\text{-}1,3\text{-}N_3)_2](ClO_4)_2$ (**1**;[29] L = *N*,*N*′,*N*″-trimethyl-1,4,7-triazacyclononane), $[(Me_5dien)_2Cu_2(\mu\text{-}1,3\text{-}N_3)_2](BPh_4)_2$ (**2**;[30] Me_5dien = 1,1,4,7,7-pentamethyldiethylenetriamine), $[(Et_5dien)_2Cu_2(\mu\text{-}1,3\text{-}N_3)_2](ClO_4)_2$ (**3**;[30, 31] Et_5dien = 1,1,4,7,7-pentaethyldiethylenetriamine), $[(EtMe_4dien)_2Cu_2(\mu\text{-}1,3\text{-}N_3)_2](ClO_4)_2$ (**4**;[31] $EtMe_4dien$ = 4-ethyl-1,1,7,7-tetramethyldiethylenetriamine) and $[(Me_5dien)_2Cu_2(\mu\text{-}1,3\text{-}N_3)_2](ClO_4)_2$ (**5**).[30, 31] Hereafter, the corresponding $[(NH_3)_6Cu_2(\mu\text{-}1,3\text{-}N_3)_2]^{2+}$ structures are labelled ete-**1** to ete-**5**.

The copper ions in the end-on-coordinated complexes are usually tetracoordinate. Since the external ligands in the end-on complexes are, in general, aromatic heterocyclic groups, we performed calculations on two models with the general formula $[(L)_4Cu_2(\mu\text{-}1,1\text{-}N_3)_2]^{2+}$, in which the external ligands were either ammonia, $[(NH_3)_4Cu_2(\mu\text{-}1,1\text{-}N_3)_2]^{2+}$, [eo-m($NH_3$)], or pyridine, $[(C_5H_5N)_4Cu_2(\mu\text{-}1,1\text{-}N_3)_2]^{2+}$, [eo-m($C_5H_5N$)]. The calculations were performed on model structures of D_{2h} symmetry (see Figure 2). The geometry was symmetrised from the experimental structure of $[(L)_4Cu_2(\mu\text{-}1,1\text{-}N_3)_2]^{2+}$ (**6**; where L = *t*Bupy = *p*-*tert*-butylpyridine).[33] Finally, some calculations were performed on $[(NH_3)_4Cu_2(\mu\text{-}1,1\text{-}N_3)_2]^{2+}$ based on the experimental C_i geometry of **6**. Table 1 summarises the most significant bond lengths used in the calculations.

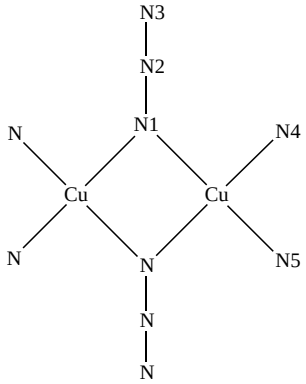

Figure 2. Schematic representation of the structure of an end-on azido-bridged Cu^{II} complex.

All electron calculations were performed by using the effective core potential for the Cu atoms determined by Barandiarán and Seijo, for which the valence electrons are described by a (3s3p4d) basis set.[48] For the bridging nitrogen atom, ANO-type functions[49] (atomic natural orbitals) were used with a (3s2p1d) contraction for the bridging nitrogen atom and a (3s2p) contraction for the terminal nitrogen atoms. An ANO (2s) basis set was used for the hydrogen atoms. In the D_{2h} eo-m(C_5H_5N) structure, a minimal basis set was used for the carbon and hydrogen atoms to make the calculation feasible.

The weak dependence of the calculated coupling constants on the basis set has already been assessed.[50–52] A verification was performed on ete-m1. We used four different basis sets for the copper and the bridging nitrogen atoms, increasing the number functions from (4s3p2d) to (5s4p3d1f) for copper and from (2s1p) to (3s2p1d) for the bridging nitrogen atoms. The variation of the calculated coupling constant at the IDDCI level is less than 11% for the four basis sets considered. More details are given in the Supporting Information.

The starting MO set has been obtained from the ROHF triplet. The two singly occupied orbitals are taken as starting active MOs.

The computational requirements, both in terms of the number of two-electron integrals and the size of the C_i spaces, are generally very high in the systems presented here. For this reason, a truncation of the MO set was applied. This dedicated molecular orbital (DMO) transformation has been used successfully in previous papers[53–56] to give a rational hierarchy of the MO set, and has allowed the MO set to be truncated by freezing the MOs that are less significant to the energy difference. The method consists of

Table 1. Relevant bond lengths used for the C_{2h} end-to-end $[(NH_3)_6Cu_2(\mu\text{-}1,3\text{-}N_3)_2]^{2+}$ complexes, ete-m1 and ete-m2, and the end-on $[L_4Cu_2(\mu\text{-}1,1\text{-}N_3)_2]^{2+}$ D_{2h} complexes, with L = NH_3, eo-m(NH_3), and L = C_5H_5N, eo-m(C_5H_5N).

Model[a]	Interatomic distances [Å]							
	Cu–Cu	Cu–N1	Cu–N3	Cu–N4	Cu–N5	Cu–N6	N1–N2	N2–N3
ete-m1 ($\alpha = 90°$)	5.192	2.010	2.010	2.052	2.052	2.244	1.158	–
ete-m2 ($\alpha = 153°$)	5.227	1.985	2.252	2.063	2.046	2.063	1.169	–
eo-m(NH_3, C_5H_5N)	3.046	1.987	–	1.988	1.988	–	1.182	1.160

[a] See Figures 1 and 2.

taking the difference of the density matrices of the states involved in the calculation of the observable searched (here the singlet and the triplet) at a low inexpensive *CI* level, and thereafter the dedicated molecular orbitals are obtained by diagonalisation of both the doubly occupied and the virtual MO blocks without changing the active MOs. The eigenvalues give participation numbers of the dedicated MOs in the observable. Smaller participation numbers indicate that the MOs contribute less to the energy difference. The consequence is the reduction of the molecular integrals in the next steps of the calculation and the reduction of the DDCI space (a fraction of 70% of the MO set gives only 25% of the molecular integrals and 35–40% of the number of determinants). As mentioned above for the iterated orbitals, the participation numbers also give a criterion to enlarge the active space. Further details and applications can be found in reference [56].

All the calculations up to the integral transformation to molecular integrals were performed with the MOLCAS 4.1 package,[57] and the diagonalisation of the *CI*; spaces was performed with the CASDI code.[58] Both the dedicated and the iterated orbitals were obtained with the NATURAL code.[59]

Results and Discussion

End-to-end complexes

A first set of calculations was performed on the C_{2h} models of the $[(NH_3)_6Cu_2(\mu\text{-}1,3\text{-}N_3)_2]^{2+}$ complex represented in Figure 1. The two active MOs are essentially the bonding and antibonding combinations of 3d atomic orbitals of copper atoms that belong to a_u and b_g irreducible representations (IR) for ete-m1 and a_g and b_u for ete-m2. In both models, the calculated states are the ^1A_g singlet and the ^3B_u triplet.

The results of the exchange coupling calculations for the idealised models are reported in Table 2 and can be compared to the experimental data of compounds **1** and **2**, which have the most comparable structures. They show that the DDCI method correctly reproduces the sign and the trend with the α angle, which reflects the changes involved in the coordination geometry as well as the order of magnitude of the coupling constant in both models. The values of J given by the IDDCI method are very close to the experimental values of compounds **1** and **2**. The DFT J value reported in Table 2 was extracted from reference [11] by means of Equation (3), in which the S^2_{ab} value is approximated to be zero. This result shows that the B3LYP functional overestimates the J value by a factor of 2. The reason for this overestimation has been shown[60] to arise from an excessive delocalisation between the metal and the ligands. A better agreement in the coupling constant can be reached by increasing the Fock contribution in the DFT functional.

The structure of the experimental complexes **1**, **2**, **4** and **5** structures transform following the C_i point group, and **3** has no inversion centre and transforms following C_1. The active orbitals are comparable to those of the C_{2h} models. The calculated states are the singlet ^1A_g and the triplet ^3A_u for the centrosymmetric ete-**1**, ete-**2**, ete-**4** and ete-**5** structures and the singlet and the triplet $^{1,3}A$ for ete-**3**. Table 2 reports all the calculated IDDCI values of the exchange coupling constant with the experimental geometries and show that the results are all in excellent agreement with experiment. Although the B3LYP value for **1** and **5** were calculated by explicitly considering the external ligands,[11] the DFT calculations overestimate the experimental value for **1** if the correct expression for the extraction of the magnetic coupling constant is used, as discussed above, and gives an incorrect sign for **5**.

End-on complexes

Use of the minimal CAS: The starting point of the DDCI calculation of the eo-m(NH_3) and eo-m(C_5H_5N) complexes is the definition of the active MOs. If the usual minimal CAS(2,2) is used, the two active MOs are the bonding and antibonding linear combinations of almost $3d_{xy}$ (also referred as $d_{x^2-y^2}$ in some works) magnetic orbitals of copper atoms that belong to the b_{2g} and b_{3u} IR. The states to be calculated are the $^1A_{1g}$ singlet and the $^3B_{1u}$ triplet. The DDCI results with the minimal CAS are shown in Table 3 for the D_{2h} models, eo-m(NH_3) and eo-m(C_5H_5N). The coupling calculated with the starting ROHF MOs (J_{DDCI}) is ferromagnetic, in agreement

Table 3. DDCI exchange coupling constant J[cm^{-1}], for end-on structures calculated with a CAS(2,2) or a CAS(6,4) model space. DFT and experimental values are listed for comparison.

Structure	CAS(2,2)		CAS(6,4)			
	J_{DDCI}	J_{IDDCI}	J_{DDCI}	J_{IDDCI}	J_{DFT}	J_{exp}[e]
eo-m(NH_3)	70	216	58	88	-141[a], -22[b], 123[c]	
eo-m(C_5H_5N)	36	265	57	82		
eo-(NH_3)	79	214	65	85	-6[b]	
eo-(C_5H_5N)					53[b]	
6					191[d]	52 ± 12

[a] Ref. [17], B3LYP. [b] Ref. [17], MPW1PW. [c] Ref. [18], B3LYP. [d] Ref. [8]. The DFT results have been obtained using B3LYP functional and Equation (3). [e] Ref. [33] and [34].

Table 2. DDCI exchange coupling constant, J[cm^{-1}], for different end-to-end structures of general formula $[(NH_3)_6Cu_2(\mu\text{-}1,3\text{-}N_3)_2]^{2+}$. DFT and experimental values are listed for comparison.

Compound[a]	Model	α[°]	J_{DDCI}	J_{IDDCI}	J_{DFT}	J_{exp}
	ete-m1	90	-401	-563	-1036[b]	–
	ete-m2	153	-14	-12	–	–
$[L_2Cu_2(\mu\text{-}1,3\text{-}N_3)_2](ClO_4)_2$	ete-1	85.3	-461	-623	-1270[b]	< -400[c]
$[(Me_5dien)_2Cu_2(\mu\text{-}1,3\text{-}N_3)_2](BPh_4)_2$	ete-**2**	153.1	-11	-11	–	-6.5[d]
$[(Et_5dien)_2Cu_2(\mu\text{-}1,3\text{-}N_3)_2](ClO_4)_2$	ete-**3**	149–152	-6	-5	–	-11.1[c], -14.0[e]
$[(EtMe_4dien)_2Cu_2(\mu\text{-}1,3\text{-}N_3)_2](ClO_4)_2$	ete-**4**	154.1	-5	-4	–	-1.8[e]
$[(Me_5dien)_2Cu_2(\mu\text{-}1,3\text{-}N_3)_2](ClO_4)_2$	ete-**5**	156.5	-6	-1	6.6[b]	-3.1[d], -3.75[e]

[a] L = *N*,*N*′,*N*″-trimethyl-1,4,7-triazacyclononane, Me_5dien = 1,1,4,7,7-pentamethyldiethylenetriamine, Et_5dien = 1,1,4,7,7-pentaethyldiethylenetriamine, $EtMe_4dien$ = 4-ethyl-1,1,7,7-tetramethyldiethylenetriamine. [b] Ref. [11]. J_{DFT} extracted using B3LYP functional and Equation (3). The external ligands are taken into account in the structure. [c] Ref. [29]. [d] Ref. [30]. [e] Ref. [31].

with the experimental value, $J_{exp} = 52 \pm 12\ cm^{-1}$. However, we observe an important dependence of the result on the external ligands, 70 cm^{-1} for eo-m(NH_3), the model with NH_3 ligands, and 36 cm^{-1} for aromatic pyridine ligands in eo-m(C_5H_5N). In spite of this difference, both results seem to be approximately inside the experimental error range. Unfortunately, when iterating the molecular orbitals with the IDDCI procedure, the previous results are proven to be fortuitous since the converged J values are increased by factors of 3 (NH_3) to 7 (C_5H_5N). In spite of the overestimation, this result advantageously compares with the DFT ones[17] also reported in Table 3 since at least the coupling is predicted to be ferromagnetic. Although the dependence on the modelling of the external ligands seems to be less important, the results cannot be conclusive because of the large overestimation.

Although the distortions of the experimental C_i structure are not very important compared to the D_{2h} symmetrised model, the coupling constant was also calculated for the C_i eo-(NH_3) structure, where the experimental distances and angles of **6**[33] were preserved. As shown in Table 3 for this structure, the J values are 79 cm^{-1} with ROHF orbitals and 214 cm^{-1} with IDDCI orbitals, compared with 70 cm^{-1} and 216 cm^{-1}, respectively, for the D_{2h} model. As expected from the small deviations from ideal D_{2h} structure, the difference in the values is not significant and proves that the overestimation cannot be attributed to a different geometry.

Since the IDDCI results indicate a small role of the modelling of the external ligands, some additional exploratory calculations on the D_{2h} eo-m(NH_3) and eo-m(C_5H_5N) and the C_i eo-(NH_3) models at a level that also allows the calculation of the distorted experimental geometry of eo-(C_5H_5N) (the model with the C_i experimental geometry and pyridine external ligands) were carried out to confirm this preliminary trend. CASPT2[57] calculations have been proven to give good results for magnetic coupling in many systems, reproducing the sign and the order of magnitude.[61] CASPT2 calculations with a (2,2) active space were performed on the four end-on models mentioned above with different basis sets. The calculated J range was between 100 and 111 cm^{-1} for the four models and basis sets considered. These results confirm that neither the symmetrisation of the molecule, nor the modelling of the external ligands by NH_3, nor the size of the basis set have a significant influence on J. Furthermore, it indicates that the strong dependence of the coupling on the external ligands is a peculiarity of DFT calculations more than a general trend. Again, the large delocalisation of the magnetic DFT orbitals explains this behaviour.

From all these considerations, we conclude that important physical effects caused by to the bridging ligand are missing in the end-on complexes and that the problem needs a more careful analysis.

Analysis of the magnetic orbitals: The shape of the magnetic orbitals has been shown to be relevant in the quantitative evaluation of J,[60] and the electron correlation induces important changes in this shape. The active orbitals are mainly the bonding and antibonding combinations of the copper d orbital directed to the ligands with some antibonding tails on the bridging and external ligands. Figure 3 shows the active orbitals for eo-m(NH_3) both at the ROHF and at the IDDCI level from a CAS(2,2) model space.

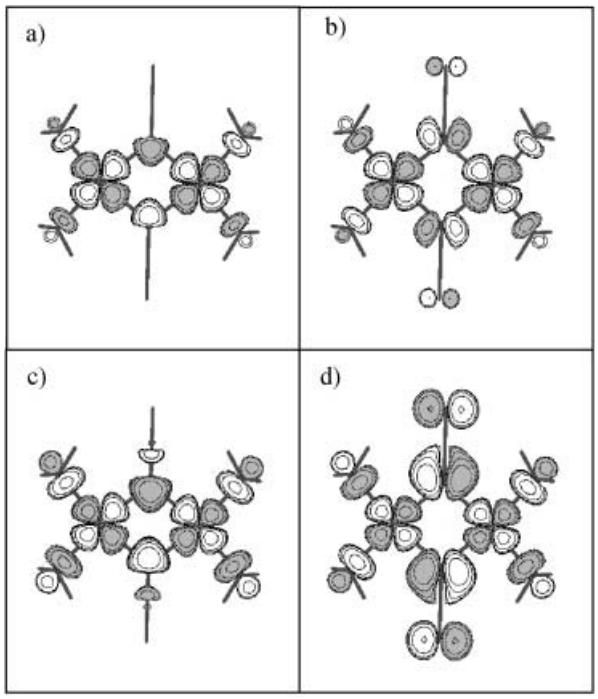

Figure 3. Magnetic orbitals of $[(NH_3)_4Cu_2(\mu\text{-}1,1\text{-}N_3)_2]^{2+}$ [eo-m(NH_3)]: a), b) ROHF orbitals; c), d) IDDCI orbitals.

The ROHF magnetic orbitals (Figure 3a, b) are concentrated on the metal atoms, and the antibonding tails on the bridging ligands are relatively small. This is a typical feature of Hartree–Fock orbitals.[60] On the other hand, the IDDCI active orbitals (Figure 3c, d) are much more delocalised on the bridging ligands with an exceptional contribution of the azido bridge π_g orbital, which is larger than the delocalisation observed in other bridged systems. The same trend is found when the external ligand is changed from NH_3 to pyridine in eo-m(C_5H_5N). This indicates that the shape of the orbitals is not significantly changed by the external ligand. This large delocalisation of the active orbitals is discussed below.

Spin densities: In ferromagnetic systems it is possible to experimentally evaluate the spin densities, which show the distribution of the unpaired electrons over the molecule. Spin densities can easily be obtained from *CI* and DFT calculations. Since the spin densities of $[(t\text{Bupy})_4Cu_2(\mu\text{-}1,1\text{-}N_3)_2](ClO_4)_2$ (**6**) obtained from polarised neutron diffraction experiments have been reported,[34] they can provide an excellent test for theoretical calculations. The spin densities from the CAS(2,2)*DDCI wave functions have been calculated from the difference between the alpha and beta spin densities for eo-m(NH_3) and eo-m(C_5H_5N) and are reported in Table 4. The DDCI column lists the spin densities calculated with the starting ROHF orbitals, while the IDDCI one corresponds to iterated NOs. The comparison of the spin densities on the most significant atoms, copper and bridging nitrogen (N1), corroborate the previous discussion on the role of the correlation on the orbital shapes, showing a larger delocalisa-

Table 4. DDCI spin densities of the $[(L)_4Cu_2(\mu\text{-}1,1\text{-}N_3)_2]^{2+}$ D_{2h} models, where $L = NH_3$, eo-m(NH_3), and $L = C_5H_5N$, eo-m(C_5H_5N), calculated with ROHF orbitals (DDCI) and iterated natural orbitals (IDDCI), and a CAS(2,2) model space. Experimental values are reported for comparison.

	eo-m(NH_3)		eo-m(C_5H_5N)		**6**
Atom [a]	DDCI	IDDCI	DDCI	IDDCI	Exp.[b]
Cu	0.761	0.704	0.731	0.689	0.783
N1	0.084	0.106	0.108	0.125	0.069
N2	0.001	0.004	−0.002	0.003	−0.016
N3	0.050	0.067	0.063	0.077	0.057
N4	0.058	0.066	0.049	0.052	0.067
N5	0.058	0.066	0.049	0.052	0.049

[a] See Figure 2. [b] Spin densities extracted from the experimental geometry and external ligand *t*Bupy = *p-tert*-butylpyridine, Ref. [34].

tion in the IDDCI spin densities caused by the weighting of the π bridge orbitals in the natural magnetic orbitals (Figure 3). Nevertheless, a comparison with the experimental results shows that both series of calculations result in spin densities that are too delocalised. Again, the external ligand is not responsible for this behaviour since the spin densities show a similar behaviour in eo-m(NH_3) and eo-m(C_5H_5N). Calculations on the C_i eo-(NH_3) model have already shown that the small changes in the geometry do not significantly change the calculated spin densities.

Role of the bridge orbitals: As indicated above, dedicated molecular orbitals (DMO)[56] provide information about the role of orbitals beyond the active subset in the value of *J* through the participation numbers. Since the singlet and triplet density matrices are not very different, these numbers are usually very small. When the DMO transformation is performed after DDCI with the CAS(2,2) model space, it is found that the most participating DMOs are π_g and π_u of the azido bridge, that is, combinations of the highest occupied nonbonding π orbitals of the N_3^- ligands, schematically represented in Figure 4.

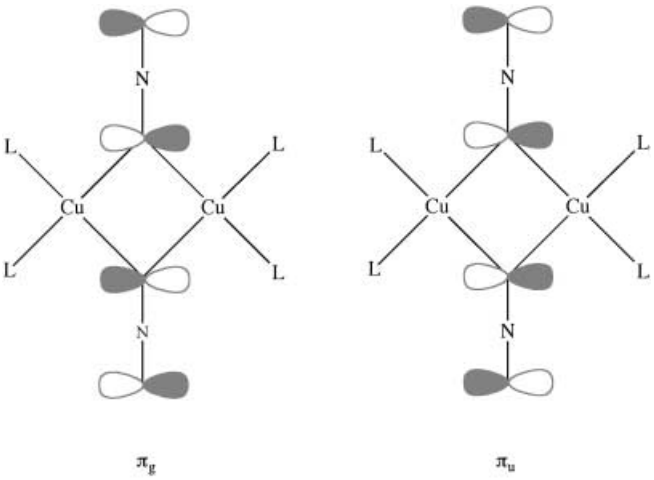

Figure 4. Schematic representation of the π_g and π_u azido bridge orbitals.

The absolute participation numbers are $p_{\pi g} = 3.90 \times 10^{-3}$ and $p_{\pi u} = 0.84 \times 10^{-3}$ in the eo-m(NH_3) complex and $p_{\pi g} = 3.58 \times 10^{-3}$ and $p_{\pi u} = 0.83 \times 10^{-3}$ in eo-m(C_5H_5N). In both cases, all the remaining participation numbers are at least one order of magnitude smaller ($< 1.1 \times 10^{-4}$). The sum of the participation numbers $p_{\pi g} + p_{\pi u}$ represents a fraction of 40% of the overall sum for both models.

The occupation numbers of NOs give complementary information, especially for iterated averaged NOs (IDDCI) that are independent of the starting MOs. Both the π_g and the π_u IDDCI orbitals have occupations significantly lower than all other doubly occupied orbitals: in the eo-m(NH_3) complex, $n_{\pi g} = 1.978$ and $n_{\pi u} = 1.992$ and in eo-m(C_5H_5N), $n_{\pi g} = 1.974$ and $n_{\pi u} = 1.990$.

These observations strongly suggest an important role of these bridge–ligand orbitals. The exceptionally strong ligand–metal delocalisation contribution from the dynamical correlation may be understood when considering the main contributions to the electron correlation introduced at the CAS(2,2)*DDCI level, namely the dynamical polarisation and the spin polarisation. The dynamical polarisation is the response of the inactive electrons to the instantaneous electric field of the active electrons in the ionic VB structures and in the ligand-to-metal charge-transfer states. Both polarisation contributions involve the ligand $\pi \rightarrow \pi^*$ excitations on top of the CAS and their effect would be overestimated if the $\pi \rightarrow \pi^*$ excitation energy is underestimated. It has been shown previously for several Cu^{II} binuclear complexes (including the ete-m1 azido-bridged complex) that both contributions cause an increase of ligand–metal delocalisation in the NOs.[22a, 60] The delocalisation contribution from the dynamical correlation in the complex discussed here (see Figure 4) is unusually large compared to the previously studied complexes. This suggests that the $\pi \rightarrow \pi^*$ energy gap is underestimated in the present case. The calculation at the CAS(2,2) level of the Anderson model[3] parameters and the comparison with those of end-to-end systems give an interpretation for the excessive delocalisation. The Anderson model relates *J* to *K*, *t*, *U* by the expression given in Equation (4), where *K* is the direct exchange term, *t* is the hopping integral and *U* is the on-site repulsion.

$$J = K - \frac{2t^2}{U} \tag{4}$$

Table 5 reports these parameters calculated as described in reference [22b] with ROHF and DDCI NOs for eo-m(NH_3), ete-m1 and ete-m2.

In eo-m(NH_3), the ferromagnetic contribution, *K*, calculated with ROHF MOs, is almost identical to *J* at the CAS(2,2) *CI* level and of the same order of magnitude as *J* at the DDCI level ($K = 39$, $J_{CAS} = 34$ and $J_{DDCI} = 70\ cm^{-1}$). The Anderson term $2t^2/U$ is small ($-5\ cm^{-1}$). Hence, the leading term is the direct exchange and the final balance is a ferromagnetic coupling at the CAS(2,2) *CI* level. In ete-m1, *K* is much smaller ($6\ cm^{-1}$) and now the leading term is the Anderson contribution ($-47\ cm^{-1}$) giving an antiferromagnetic *J* at the CAS(2,2) *CI* level. The underestimation of *J* by one order of magnitude compared to J_{DDCI} indicates that an important part of the physics is missing at this zeroth-order level.

After including the dynamical correlation in the IDDCI active orbitals, these parameters change dramatically. In eo-

Table 5. Magnetic parameters: direct exchange K, Anderson's antiferromagnetic contribution $-2t^2/U$, and coupling constant J [cm^{-1}] at the CAS(2,2) *CI* level with different types of molecular orbitals in different models. The spin polarisation SP, and the remaining dynamical correlation effects DC,[a] are also reported for ROHF orbitals.

Model	Orbital set	K	$-2t^2/U$	$J_{CAS(2,2)}$	SP	DC[a]	J_{DDCI}	J_{exp}
eo-m(NH_3)	ROHF MOs	39	−5	34	63	−27	70	52 ± 12
	IDDCI(2,2) NOs	732	−184	548			216	
	IDDCI(6,4) NOs	328	−85	243			88[b]	
ete-m1	ROHF MOs	6	−47	−41	−30	−330	−401	< -400
	IDDCI(2,2) NOs	360	−490	−130			−563	
ete-m2	ROHF MOs	1	−2	−1	0	−13	−14	−6.5
	IDDCI(2,2) NOs	58	−33	25			−12	

[a] $DC = J_{DDCI} - J_{CAS} - SP$. [b] The DDCI value was obtained with the enlarged CAS(6,4) model space.

m(NH_3), K and t are multiplied by large factors and the on-site repulsion U is reduced, according to the extremely large delocalisation of the magnetic orbitals. The Anderson term is multiplied by a factor 40, while in the end-to-end models, ete-m1 and ete-m2, this term is only multiplied by a factor of 10–16.

We may conclude that the probable origin of these over-estimated effects is the underestimation of $\pi \rightarrow \pi^*$ energy gap of the azido group, or equivalently, that the π_g and π_u orbitals have too high an energy in the complex at the CAS(2,2) level. These two orbitals are the bonding combination of the singly occupied orbitals of the metal and the non-bonding π orbitals of the azido ligands. It is easy to understand that this problem is less significant in the end-to-end coordination mode, as is verified below, because the larger overlap and the interaction in the latter case cause these two orbitals to have lower orbital energy.

We conclude that the correlation of the azido ligand has to be included in the calculation through the $\pi_{g,u}{}^2 \rightarrow \pi^{*2}$ excitations. As discussed in above, the usual DDCI procedure includes the products of the minimal CAS(2,2) configuration by the double excitation processes including at least one active orbital. This means that, although excitations coming from both π_g and π_u orbitals belong to the DDCI space, double excitations from these orbitals to the corresponding combinations of π^* orbitals of the azido ligands are not included since these configurations imply four inactive orbitals. Enlarging the CAS with the π_g and π_u orbitals allows us to include these important electron-correlation effects.

Adding the $\pi^2 \rightarrow \pi^{*2}$ configurations of the azido-bridge: A new set of calculations was carried out on the D_{2h} eo-m(NH_3) and eo-m(C_5H_5N) models enlarging the CAS with the π_g and π_u bridge orbitals to give a model space with six electrons and four active orbitals, CAS(6,4). The occupation numbers of the π_g and π_u IDDCI natural orbitals are very similar and significantly lower than in the precedent calculation, $n_{\pi g} = n_{\pi u} = 1.945$ and $n_{\pi g} = n_{\pi u}$ 1.942 for eo-m(NH_3) and eo-m(C_5H_5N), respectively. This indicates that the bridge $\pi^2 \rightarrow \pi^{*2}$ correlation indeed plays a very important role. The exchange coupling constants with the CAS(6,4) model space are shown in Table 3 for both models obtained with the starting ROHF orbitals (J_{DDCI}) and the natural orbitals (J_{IDDCI}), respectively. The J value at the DDCI level shows a good agreement with experiment and there is no evident dependence on the external ligand modelling (58 cm^{-1} with L = NH_3 and 57 cm^{-1} with L = pyridine). The final IDDCI results are 88 cm^{-1} with L = NH_3 and 82 cm^{-1} with L = pyridine. The DFT values are reported in Table 3 for comparison. As previously mentioned, these results are very sensitive to the functional and to the modelling of the external ligands. In general, all DFT results are unable to reproduce the J value and sometimes even fail to predict the ferromagnetic character of the eo-m(NH_3) model. For this model, the J values reported in references [17] and [18] calculated with the B3LYP functional have opposite signs (see Table 3). This is probably caused by to slight differences in geometries and basis sets. Only the MPW1PW functional[17] gives on eo-(C_5H_5N) J = 53 cm^{-1}, in excellent agreement with experiment, 52 ± 12 cm^{-1}, although the spin densities are considerably underestimated on the metal. The spin densities have been recalculated with IDDCI NOs and the CAS(6,4) model space. The results reported in Table 6 are in excellent agreement with the polarised neutron diffraction spin densities.[34] This smaller delocalisation of the magnetic orbitals also has consequences with regard to the magnetic parameters. Table 5 reports these parameters at the CAS(2,2) level for the natural orbitals from CAS(6,4)*IDDCI. The factor 17 between the Anderson term and the corresponding value obtained with ROHF MOs is now close to those found in ete-m1 and ete-m2. The effect on K is also significant because the value is about one half of the CAS(2,2)*IDDCI one.

Table 6. DDCI spin densities of the $[(L)_4Cu_2(\mu\text{-}1,1\text{-}N_3)_2]^{2+}$ D_{2h} models, where L = NH_3, eo-m(NH_3), and L = C_5H_5N , eo-m(C_5H_5N), calculated with iterated natural orbitals (IDDCI) and a CAS(6,4) model space. DFT calculations and experimental values are also reported.

	eo-m(NH_3)		eo-m(C_5H_5N)		**6**	
Atom[a]	IDDCI	MPW1PW[b], [d]	IDDCI	BP[c], [e]	B3LYP[e], [f]	Exp.[c], [e]
Cu	0.774	0.57	0.773	0.425	0.60	0.783
N1	0.074	0.15	0.08	0.167	0.14	0.069
N2	0.003	−0.04	0.004	−0.005	−0.04	−0.016
N3	0.044	0.12	0.045	0.122	0.12	0.057
$N4_4$	0.057	0.11	0.045	0.129	0.09	0.067
N5	0.057	0.11	0.045	0.120	0.09	0.049

[a] See Figure 2. [b] Spin densities extracted from the modelled geometry and external ligand NH_3. [c] Spin densities extracted from the experimental geometry and external ligand *t*Bupy = *p-tert*-butylpyridine. [d] Ref. [17]. [e] Ref. [34]. [f] Ref. [8].

Effects on end-to-end systems of the azido-bridge $\pi^2 \rightarrow \pi^{*2}$ correlation

Since the end-to-end calculations were performed with the simple CAS(2,2) model space, it is necessary to verify that the good results were not fortuitous and that the results are stable against the introduction of the bridge $\pi^2 \rightarrow \pi^{*2}$ correlation.

For this purpose, a new set of calculations was performed in the end-to-end systems to test the role of the π_g and π_u bridge orbitals of the azido groups in the value of the magnetic coupling constant. For this test, the ete-m2 model was used with an active space of four orbitals and six electrons. The J value at DDCI level is $-11\ cm^{-1}$ compared to $-14\ cm^{-1}$ for the minimal CAS (Table 2). The IDDCI J value is $-9\ cm^{-1}$ instead of the $-12\ cm^{-1}$ obtained with the minimal CAS as the model space. In both cases (ROHF or natural orbitals), the enlarged CAS only moderately affects the J values, which are 75–80% of the values obtained with the minimal CAS. This indicates that the bridge correlation has a minor effect on the end-to-end systems.

Comparing the end-to-end versus the end-on coordination

The different magnetic role of both types of bridges deserves an analysis to understand the different sign of the coupling. As previously indicated, the two main contributions of the dynamical correlation to the coupling constant are the dynamical polarisation and the spin polarisation. The spin polarisation (SP) can result in both ferromagnetic and antiferromagnetic contributions. Its sign can be rationalised by the Ovchinnikov rule[62] and is verified by Charlot et al.[36] from a Heisenberg Hamiltonian model that includes the non-bonding HOMO and the antibonding LUMO π orbitals of the N_3^- ligand. This contribution is ferromagnetic for end-on coordination and antiferromagnetic for end-to-end coordination. Here we explicitly evaluate the spin polarisation in both coordination modes by including only those configurations in the *CI* responsible for this effect. We not only calculate the *SP* arising from those orbitals considered by Charlot et al., but we also include the effect of all core and virtual orbitals. The remaining dynamical correlation (DC) effects that include the relaxation of the ionic and ligand-to-metal charge-transfer configurations among other less important terms, always give an antiferromagnetic contribution to the coupling.[22a] These two main contributions to the DC are evaluated by subtracting SP and J_{CAS} from J_{DDCI}.

The results reported in Table 5 give the values of the K, $2t^2/U$, and the SP and DC contributions. For the eo-m(NH_3) with ROHF orbitals, the most important contribution to the sign of J_{DDCI} are the direct exchange and the spin polarisation, 39 and $63\ cm^{-1}$, respectively. In this case, the spin polarisation is positive and stabilises the triplet state to give 90% of $J = 70\ cm^{-1}$ at the DDCI level. This result is in agreement with the interpretation of Charlot et al.[36] on the origin of the ferromagnetic coupling; however, it is in contrast to the VBCI calculation[35] that gives a negative contribution for the effects that go beyond the direct exchange. The remaining DC effects are rather small contributing with $-27\ cm^{-1}$ to J.

The same contributions have been calculated in two end-to-end complexes, ete-m1 and ete-m2, with ROHF orbitals. Because of the large Cu–Cu distance, the direct exchange is very small in this systems, 6 and $1\ cm^{-1}$, respectively. All the remaining contributions are antiferromagnetic. As expected from the Ovchinnikov rule, the spin polarisation contribution is negative for ete-m1, $-30\ cm^{-1}$, and almost zero for ete-m2. This contribution does not confirm the result given by the phenomenological model[36] since it is far from being the determining factor of the antiferromagnetic coupling of this coordination mode. The leading factor is the strongly negative contribution of the remaining dynamical correlation effects. As shown previously in other antiferromagnetic systems,[21, 22a, 63] the relaxation of the ligand-to-metal charge-transfer configurations brings an important part of this negative contribution. In the complete calculation of J, these effects are not additive but their qualitative role is preserved.

Conclusion

The end-to-end and end-on coordination modes of the azido bridge in binuclear Cu^{II} compounds has been analysed by means of the DDCI approach. In the end-to-end complexes, the coupling is found to be antiferromagnetic and the magnitude is in agreement with the experimental data. Because of the long Cu–Cu distance, direct exchange is low in this type of complex and the remaining contributions, particularly the spin polarisation and especially the dynamical polarisation of the ionic and ligand-to-metal charge-transfer configurations, are the most important ones to stabilise the singlet state.

The end-on coordination is very sensitive to a correct valence description of the bridging ligand to ensure a correct metal–ligand delocalisation. The ferromagnetic coupling is partly caused by a larger direct exchange because of a shorter Cu–Cu distance, but mostly to a positive contribution of the spin polarisation that stabilises the triplet state. When including the electron correlation to give the proper delocalisation, a good coupling constant and spin densities are obtained that are in excellent agreement with polarised neutron diffraction results.

Finally, the external ligand modelling seems to play a minor role in the ab initio, highly correlated description of the magnetic coupling. This disagreement with some DFT descriptions may be interpreted through the overestimation of delocalisation given by these functionals resulting in a major sensibility to the role of the metal surroundings.

Acknowledgement

The authors are grateful to C. J. Calzado for many comments and suggestions, and are indebted to the Catalan–French scientific cooperation (PICS2001-13). The Rovira i Virgili University authors thank the Spanish Ministry of Science and Technology (Project BQU2002-04029-C02-02) and the DURSI of the Generalitat de Catalunya (grant SGR01-00315) for their financial support. The Laboratoire de Physique Quantique is Unité Mixte (UMR 5626) du CNRS.

[1] J. Girerd, O. Kahn, M. Verdaguer, *Inorg. Chem.* **1980**, *19*, 274–276.
[2] R. D. Willett, in *Magneto Structural Correlations in Exchange Coupled Systems*, NATO, Advanced Studies Ser. C, *Vol. 140*, (Eds.: R. D. Willet, D. Gatteschi, O. Kahn), Reidel, Dordrecht, **1985**, pp. 389–420; see also D. N. Hendrickson and W. E. Hatfield in *Magneto Structural Correlations in Exchange Coupled Systems*, NATO, Advanced Studies Ser. C, *Vol. 140*, (Eds.: R. D. Willet, D. Gatteschi, O. Kahn), Reidel, Dordrecht, **1985**, pp. 523–554 and pp. 555–602, respectively.

[3] a) P. W. Anderson, *Phys. Rev.* **1950**, *79*, 350–356; b) P. W. Anderson, in *Theory of the Magnetic Interaction: exchange in insulators and superconductors*, *Solid State Phys.*, *Vol. 14*, (Eds.: F. Turnbull, F. Seitz), Academic Press, New York, **1963**, pp. 99–124.
[4] P. J. Hay, J. C. Thibeault, R. Hoffmann, *J. Am. Chem. Soc.* **1975**, *97*, 4884–4899.
[5] O. Kahn, B. Briat, *J. Chem. Soc. Faraday Trans. 2* **1976**, *72*, 268–281.
[6] S. Alvarez, M. Julve, M. Verdaguer, *Inorg. Chem.* **1990**, *29*, 4500–4507.
[7] E. Ruiz, P. Alemany, S. Alvarez, J. Cano, *J. Am. Chem. Soc.* **1997**, *119*, 1297–1303.
[8] E. Ruiz, J. Cano, S. Alvarez, P. Alemany, *J. Am. Chem. Soc.* **1998**, *120*, 11122–11129.
[9] J. Cano, P. Alemany, S. Alvarez, M. Verdaguer, E. Ruiz, *Chem. Eur. J.* **1998**, *4*, 476–484.
[10] S. Ferlay, T. Mallah, R. Ouahès, P. Vellet, M. Verdaguer, *Inorg. Chem.* **1999**, *38*, 229–234.
[11] F. Fabrizi de Biani, E. Ruiz, J. Cano, J. J. Novoa, S. Alvarez, *Inorg. Chem.* **2000**, *39*, 3221–3229.
[12] P. de Loth, P. Cassoux, J. P. Daudey, J. P. Malrieu, *J. Am. Chem. Soc.* **1981**, *103*, 4007–4016.
[13] M. Charlot, M. Verdaguer, Y. Journaux, P. de Loth, J. P. Daudey, *Inorg. Chem.* **1984**, *23*, 3802–3808.
[14] a) L. Noodleman, J. G. Norman, Jr., *J. Chem. Phys.* **1979**, *70*, 4903–4906; b) L. Noodleman, *J. Chem. Phys.* **1981**, *74*, 5737–5743.
[15] R. L. Martin, F. Illas, *Phys. Rev. Lett.* **1997**, *79*, 1539–1542.
[16] F. Illas, R. L. Martin, *J. Chem. Phys.* **1998**, *108*, 2519–2527.
[17] C. Adamo, V. Barone, A. Bencini, F. Totti, I. Ciofini, *Inorg. Chem.* **1999**, *38*, 1996–2004.
[18] C. Blanchet-Boiteux, J. M. Mouesca, *J. Am. Chem. Soc.* **2000**, *122*, 861–869.
[19] J. Miralles, O. Castell, R. Caballol, J. P. Malrieu, *Chem. Phys.* **1993**, *172*, 33–43.
[20] J. Miralles, J. P. Daudey, R. Caballol, *Chem. Phys. Lett.* **1992**, *198*, 555–562.
[21] J. Cabrero, N. Ben Amor, C. de Graaf, F. Illas, R. Caballol, *J. Phys. Chem. A* **2000**, *104*, 9983–9989.
[22] a) C. J. Calzado, J. Cabrero, J. P. Malrieu, R. Caballol, *J. Chem. Phys.* **2002**, *116*, 2728–2747. b) C. J. Calzado, J. Cabrero, J. P. Malrieu, R. Caballol, *J. Chem. Phys.* **2002**, *116*, 3985–4000.
[23] C. de Graaf, I. de P. R. Moreira, F. Illas, R. L. Martin, *Phys. Rev. B* **1999**, *60*, 3457–3464.
[24] D. Muñoz, F. Illas, I. de P. R. Moreira, *Phys. Rev. Lett.* **2000**, *84*, 1579–1582.
[25] C. de Graaf, F. Illas, *Phys. Rev. B* **2001**, *63*, 014404.
[26] I. de P. R. Moreira, D. Muñoz, F. Illas, C. de Graaf, M. A. Garcia-Bach, *Chem. Phys. Lett.* **2001**, *345*, 183–188.
[27] J. Comarmond, P. Plumeré, J. M. Lehn, Y. Agnus, R. Louis, R. Weiss, O. Kahn, I. Morgensten-Badarau, *J. Am. Chem. Soc.* **1982**, *104*, 6330–6340.
[28] O. Kahn, S. Sikorav, J. Gouteron, S. Jeannin, Y. Jeannin, *Inorg. Chem.* **1983**, *22*, 2877–2883
[29] P. Chaudhuri, K. Oder, K. Wieghardt, B. Nuber, J. Weiss, *Inorg. Chem.* **1986**, *25*, 2818–2824.
[30] T. R. Felthouse, D. N. Hendrickson, *Inorg. Chem.* **1978**, *17*, 444–456.
[31] A. Escuer, M. Font-Bardía, E. Peñalba, X. Solans, R. Vicente, *Inorg. Chim. Acta* **2000**, *298*, 195–201.
[32] A. Escuer, M. A. S. Goher, F. A. Mautner, R. Vicente, *Inorg. Chem.* **2000**, *39*, 2107–2112.
[33] S. Sikorav, L. Bkouche-Waksman, O. Kahn, *Inorg. Chem.* **1984**, *23*, 490–495.
[34] M. A. Aebersold, B. Gillon, O. Plantevin, L. Pardi, O. Kahn, P. Bergerat, I. von Seggern, F. Tuczek, L. Öhrström, A. Grand, E. Lelièvre-Berna, *J. Am. Chem. Soc.* **1998**, *120*, 5238–5245.
[35] I. von Seggern, F. Tuczek, W. Bensch, *Inorg. Chem.* **1995**, *34*, 5530–5547.
[36] M.-F. Charlot, O. Kahn, M. Chaillet, C. Larrieu, *J. Am. Chem. Soc.* **1986**, *108*, 2574–2581.
[37] E. I. Solomon, F. Tuczek, C. Brown, D. Root, *Chem. Rev.* **1994**, *94*, 827-
[38] a) W. Heisenberg, *Z. Phys.* **1928**, *49*, 619–636; b) P. A. M. Dirac, *Proc. R. Soc. London A* **1929**, *123*, 714; c) P. A. M. Dirac in *The Principles of Quantum Mechanics*, Clarendon Press, Oxford, **1947**; d) J. H. Van Vleck in *The Theory of Electric and Magnetic Susceptibilities*, Oxford University Press, Oxford, **1932**.
[39] a) L. Noodleman, E. R. Davidson, *Chem. Phys.* **1986**, *109*, 131–143; b) L. Noodleman, C. Y. Peng, D. A. Case, J. M. Mouesca, *Coord. Chem. Rev.* **1995**, *144*, 199–244.
[40] R. Caballol, O. Castell, F. Illas, I. de P. R. Moreira, J. P. Malrieu, *J. Phys. Chem. A* **1997**, *101*, 7860–7866.
[41] A. A. Ovchinnikov, J. K. Labanowski, *Phys. Rev.* **1996**, *A53*, 3946–3952.
[42] O. Castell, R. Caballol, R. Subra, A. Grand, *J. Phys. Chem.* **1995**, *99*, 154–157.
[43] O. Castell, R. Caballol, *Inorg. Chem.* **1999**, *38*, 668–673.
[44] V. M. García, R. Caballol, J. P. Malrieu, *Chem. Phys. Lett.* **1996**, *261*, 98–104.
[45] V. M. García, R. Caballol, J. P. Malrieu, *J. Chem. Phys.* **1998**, *109*, 504–511.
[46] V. M. García, O. Castell, R. Caballol, J. P. Malrieu, *Chem. Phys. Lett.* **1995**, *238*, 222–229.
[47] J. Cabrero, R. Caballol, J. P. Malrieu, *Mol. Phys.* **2002**, *100*, 919–926.
[48] Z. Barandiarán, L. Seijo, *Can. J. Chem.* **1992**, *70*, 409–415.
[49] K. Pierloot, B. Dumez, P.-O. Widmark, B. O. Roos, *Theoret. Chim. Acta* **1995**, *90*, 87–114.
[50] J. Casanovas, J. Rubio, F. Illas, in: *New Challenges in Computational Quantum Chemistry* (Eds.: R. Broer, P. J. C. Aerts, P. S. Bagus), University of Groningen (The Netherlands), **1993**, p. 214.
[51] J. Casanovas, F. Illas, *J. Chem. Phys.* **1994**, *100*, 8257.
[52] N. Queralt, C. de Graaf, J. Cabrero, R. Caballol, *Mol. Phys.* in press.
[53] J. Miralles, R. Caballol, J. P. Malrieu, *Chem. Phys.* **1991**, *153*, 25–37.
[54] O. Castell, R. Caballol, V. M. García, K. Handrick, *Inorg. Chem.* **1996**, *35*, 1609.
[55] C. J. Calzado, J. F. Sanz, O. Castell, R. Caballol, *J. Phys. Chem. A* **1997**, *101*, 1716–1721.
[56] C. J. Calzado, J. P. Malrieu, J. Cabrero, R. Caballol, *J. Phys. Chem. A* **2000**, *104*, 11636–11643.
[57] MOLCAS Version 4: K. Andersson, M. R. A. Blomberg, M. P. Fülscher, G. Karlström, R. Lindh, P. Å.Malmqvist, P. Neogrády, J. Olsen, B. O. Roos, A. J. Sadlej, M. Schütz, L. Seijo, L. Serrano-Andrés, P. E. M. Siegbahn, P. O. Widmark, Lund University (Sweden), **1997**.
[58] CASDI program: N. Ben Amor, D. Maynau, *Chem. Phys. Lett.* **1998**, *286*, 211–220.
[59] NATURAL program: V. M. García, O. Castell, R. Caballol (**1995**).
[60] J. Cabrero, C. J. Calzado, D. Maynau, R. Caballol, J. P. Malrieu, *J. Phys. Chem. A*, **2002**, *106*, 8146–8155.
[61] C. de Graaf, C. Sousa, I. de P. R. Moreira, F. Illas, *J. Phys. Chem. A*, **2001**, *105*, 11371–11378.
[62] A. A. Ovchinnikov, *Theor. Chim. Acta* **1978**, *47*, 297.
[63] a) C. J. Calzado, J. F. Sanz, J. P. Malrieu, F. Illas, *Chem. Phys. Lett.* **1999**, *307*, 102–108; b) C. J. Calzado, J. F. Sanz, J. P. Malrieu, *J. Chem. Phys.* **2000**, *112*, 5158–5167.

Received: June 8, 2002
Revised: December 17, 2002 [F4167]

